

# CHARACTERIZATION OF THE GRID DESIGN BY FITTING OF THE DISTRIBUTED SERIAL GRID RESISTANCE TO CELLO RESISTANCE MAPS AND GLOBAL IV CURVES

Jürgen Carstensen, Alireza Abdollahinia, Andreas Schütt, Helmut Föll

Institute for Materials Science, Faculty of Engineering, Christian-Albrechts-University of Kiel,  
Kaiserstr. 2, 24143 Kiel, Germany, email: jc@tf.uni-kiel.de, Phone: (+49) 431 880 6181, Fax: (+49) 431 880 6178

**ABSTRACT:** CELLO results from a large number of solar cells and results from other tools sensitive to local serial resistance show unambiguously that the grid is not an equipotential layer. As a consequence, a distributed serial resistance has to be taken into account. As shown in this paper a formerly proposed model is necessary and sufficient to obtain consistent results from iv-curve analysis and CELLO resistance maps. Necessary corrections between iv-curve measurements and CELLO are taken into account and explained.

## 1 INTRODUCTION

CELLO is probably the first tool that allows a quantitative analysis of lateral serial resistance losses on large area solar cells [1, 2]. In order to extract numbers for local serial resistances from the local measurements, a better understanding of the resistance network of emitter and grid and its interaction with the pn-junction diode resistance was necessary. The validity of various models could be tested using the CELLO measurement data and this resulted in a rather simple model that can explain all experimental findings including iv-curve data of large area solar cells. According to this model the global serial resistance  $R_{ser}$  (as taken from the standard equivalent circuit) changes along the iv-curve even so  $R_{ser}$  just describes the property of a passive network of resistance elements and is thus supposed to be constant. The global serial resistance is rather given by the sum

$$R_{ser} = R_G + R_S(U) \quad (1)$$

where  $R_G$  is a constant pure ohmic resistor and  $R_S(U)$  is a voltage dependent distributed resistance which by introducing a second constant  $R_{S,\infty}$  is calculated according to

$$R_S(U) = \frac{1}{\frac{1}{R_{S,\infty}} + \frac{1}{R_D(U)}} \quad (2)$$

Here  $R_D(U)$  represents the inverse slope of the diode of the pn-junction (cf. Eq. (6)). So for correctly describing the serial resistance of a large solar cell, i.e. for correctly taking into account the distributed serial resistance only one additional parameter (compared to the standard model) must be known. It can be shown that for a perfect solar cell  $R_G = R_{S,\infty}$ , and in general  $R_G < R_{S,\infty}$ ; so the distributed part of the serial resistance can never be neglected. For a reasonably good solar cell at the working point  $R_D(U_a)$  is much larger than the serial resistance  $R_{S,\infty}$ . So for the largest part of the iv-curve  $R_{ser} \approx R_G + R_{S,\infty} = const.$  is constant indeed but in strong forward direction where  $R_D(U) \approx R_{S,\infty}$  significantly smaller numbers for  $R_S$  can be expected and are found experimentally, indeed. In this paper the procedure to incorporate the distributed serial resistance into the standard fit of the iv-curve will be discussed, and the fitting result will be compared to serial resistance data extracted from CELLO maps along the iv-curve. As will be shown,

consistent results between both sets of resistance data are only found if taking into account the distributed serial resistance in both experiments.

## 2 EXPERIMENTS

The distributed resistance of a standard mono-Si solar cell sample (12.5cm x 12.5 cm) is investigated by CELLO (section 2.1) and iv-curve measurements (section 2.2).

### 2.1 Serial resistance data extracted from CELLO maps

**Fig. 1** shows the iv-curve of the investigated solar cell. Note that for greater convenience the sign of the current  $I$  is inverted with respect to a “standard” iv-curve representation. For this cell one CELLO map of the short circuit current  $dI_{ph}$  (cf. **Fig. 2a**) and a sequence of voltage maps  $dU(I)$  for several fixed currents  $I$  (indicated by the arrows in **Fig. 1**) have been measured. According to the procedure described in [2] the ratio of the voltages and the short circuit current at each pixel is plotted as a resistance map; an example is shown in **Fig. 2c** for the voltage map measured at  $I = 3114$  mA (cf. **Fig. 2b**). Following again the procedure described in [2] serial and diode resistances can be separated just by using the information of the histogram  $H(R)$  extracted from the resistance map as follows:

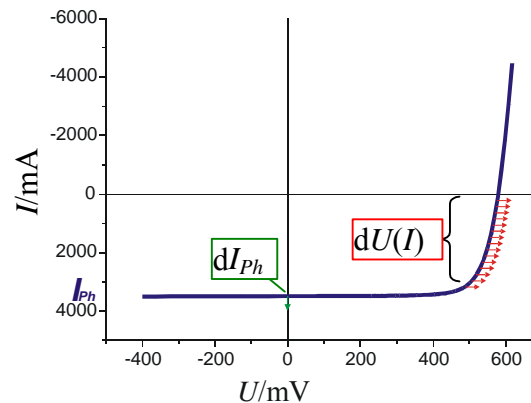


**Figure 1:** iv-curve of a standard mono Si solar cell. Potentiostatic and galvanostatic points of CELLO measurements are indicated. Note: for convenience the sign of the current  $I$  is inverted.

First calculate the integral

$$N(R) := \int_0^R H(R) dR, \quad (3)$$

and in a second step rescale the integral and take the inverse of this function via

$$x(R) := \frac{N(R)}{N(\infty)} \Rightarrow R(x). \quad (4)$$

This procedure generates the resistance distribution  $R(x)$  where  $x$  is the fraction of the solar cell area across which the current has flown to reach a certain ohmic loss. Examples for this procedure for three resistance maps are shown in **Fig. 3**.

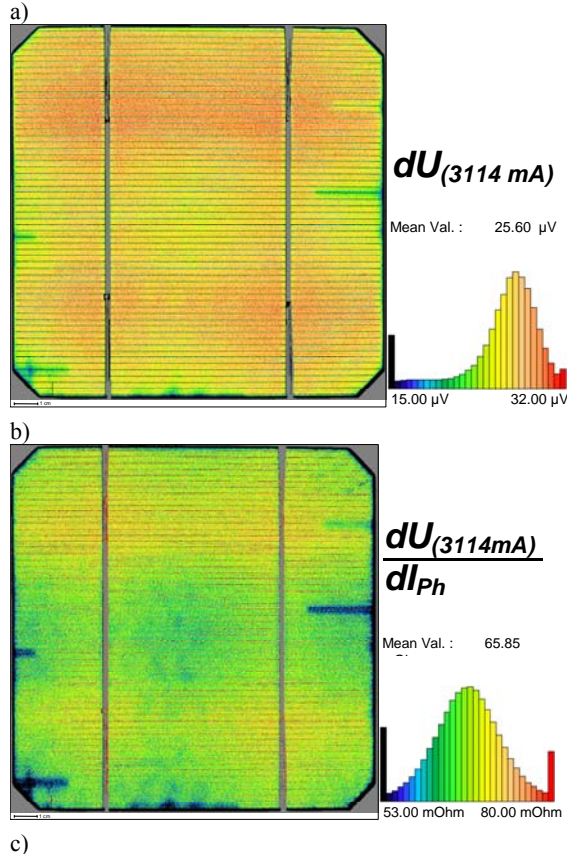
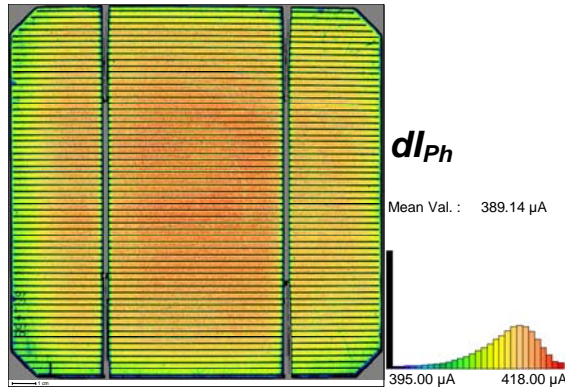


**Figure 2:** Example for CELLO maps. a) Photocurrent map  $dI_{ph}$ , b) Voltage map at the mpp; c) resistance distribution map at mpp. For details cf. text.

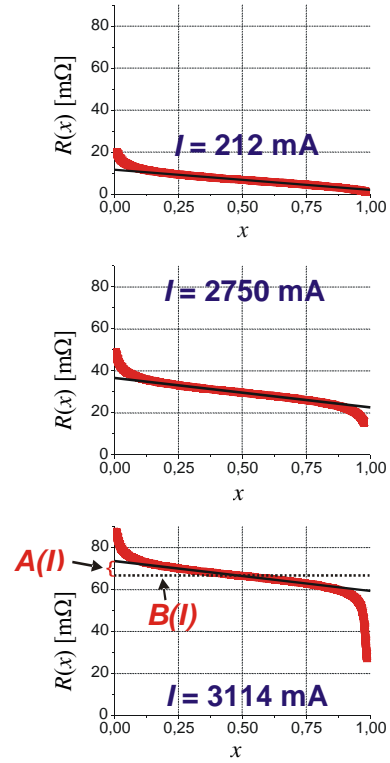


**Figure 3:**  $R(x)$  for different  $I$ .  $A(I)$  represents the slope and  $B(I)$  the average of the linear fit of  $R(x)$  (black line).

According to our theory for distributed serial resistances straight lines are expected. According to **Fig. 3** this is indeed the case for a large part of the measured curves. Deviations from the straight line do not indicate a failure of the model - the parts with the highest and smallest resistances just contain all parts with noisy data. The slope  $A$  of these straight lines equals twice the global distributed serial resistance; the average  $B$  represents the diode resistance. Both values have been fitted for the  $R(x)$  curves of all measured voltage maps; the results for  $A$  and  $B$  as a function of  $I$  are plotted in **Fig. 4** and **Fig. 5**. Note that the slope  $A$  just changes slightly while the average  $B$  changes by more than one order of magnitude. According to the current flow directions in the CELLO voltage maps the diode resistance has an offset caused by the serial resistance. Taking into account this additional offset, for the distributed serial resistance, the following equation should be expected:

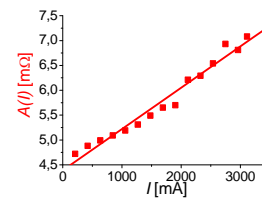


**Figure 4:**  $A(I)$  vs.  $I$  with linear fit (line).

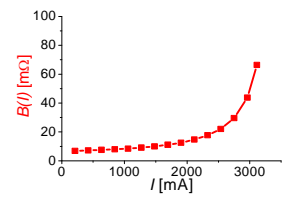


**Figure 5:**  $B(I)$  vs.  $I$ . Line to guide the eye.

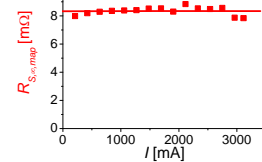


**Figure 6:**  $R_{S,\infty, \text{map}}(I)$  calculated from the curves in **Fig. 4** and **Fig. 5** according to Eq. (5).

$$\frac{1}{A(I)} = \frac{1}{R_{S,\infty, \text{map}}} + \frac{1}{A(I)+B(I)} \quad (5)$$

Using this equation to calculate  $R_{S,\infty, \text{map}}$  in Fig. 6, a nearly constant value of  $R_{S,\infty, \text{map}} = 8 \text{ m}\Omega$  is found.

## 2.2 Fit of iv-curve data

The standard two-diode model can be written as

$$I(\tilde{U}) = \tilde{I}_{01}(\tilde{U}) + \tilde{I}_{02}(\tilde{U}) + \frac{\tilde{U}}{R_{Shunt}} - I_{Ph} \quad (6a)$$

with

$$\tilde{I}_{0i}(\tilde{U}) = I_{0i} \left( \exp\left(\frac{q\tilde{U}}{n_{0i}kT}\right) - 1 \right), \quad (6b)$$

and

$$\tilde{U} = U - R_{ser} I(\tilde{U}). \quad (6c)$$

$$\frac{1}{R_D(U)} := \frac{d(\tilde{I}_{01}(U) + \tilde{I}_{02}(U))}{dU}, \quad (6d)$$

where  $I_{01}$ ,  $I_{02}$ ,  $n_{01}$ ,  $n_{02}$ ,  $R_{Shunt}$ ,  $I_{Ph}$ , are fitting parameters with the standard interpretation. Replacing the constant  $R_{ser}$  by two fitting parameters  $R_G$  and  $R_{S,\infty, iv}$  using Eq. (1) and (2), the distributed serial resistance can be easily incorporated in the two diode (or any other) model. Applying this model to the iv-curve of **Fig. 1**,  $R_S$  and  $R_D$  can be calculated from the fitting parameters as a function of applied voltage resp. the resulting current  $I$ . The resulting curves are shown in **Fig. 7** and **Fig. 8**. Again a nearly linear increase of the resistance is found while the diode resistance increases drastically. The values for the two fitting parameters of the serial resistance network are  $R_G \approx 2 \text{ m}\Omega$  and  $R_{S,\infty, iv} \approx 1.9 \text{ m}\Omega$ .

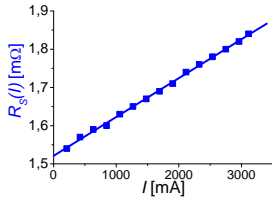


**Figure 7:**  $R_S(I)$  vs.  $I$ , linear fit.

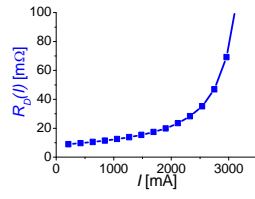


**Figure 8:**  $R_D(I)$  vs.  $I$ , line to guide the eye.

## 3 DISCUSSION

Since both types of experiments have been performed on the same solar cell one expects the same results for the numbers extracted from the measurements. Quite obviously  $R_{S,\infty, iv}$  and  $R_{S,\infty, \text{map}}$  differ by a factor of 4. This is not an error but reflects the differences in the geometry for the mapping experiments (local LASER illumination) and homogeneous illumination for the iv-curve measurements. As illustrated in **Fig. 9** this is equivalent to using 4 LASER beams illuminating symmetric points on the solar cell (the typical mirror current sources) which leads to the standard increase by a factor of 4 for the resulting resistance.

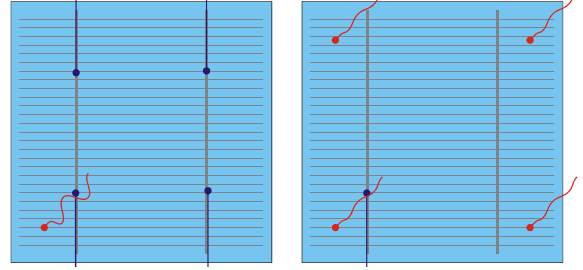


**Figure 9:** CELLO experiments use one LASER beam and typically 4 reference electrodes to emulate the necessary four-fold symmetry of typical solar cells (right). This arrangement is equivalent to using one reference electrode and illuminating 4 symmetric points on the solar cell (left).

**Fig. 10** shows the ratio between the distributed serial resistance data  $A$  extracted from the map (cf. **Fig. 4**) and the distributed serial resistance data from the fit of the iv-curve (cf. **Fig. 7**) while **Fig. 11** shows the corresponding ratio between the diode resistance data  $B+A$  extracted from the map (cf. **Fig. 5**) and the diode resistance data from the fit of the iv-curve (cf. **Fig. 8**). Both ratios should be constant but show a weak (linear) dependence on  $I$ . The ratio of the distributed serial resistance is as expected near  $0.25 = 1/4$  while the ratio of the diode resistances has values around 1. The reason for the weak linear dependence in Fig. 10 is easy to understand: the voltage maps have been divided by the short circuit current maps, which induces a small error. Not all current locally introduced into the solar cell (measured as short circuit current) will be distributed across the solar cell under forward bias; a certain fraction will be needed to build up a photo potential, leading to a correction factor for the current which generates lateral ohmic losses. Defining the function

$$F(I) = 1 - z(I_{Ph} - I) \quad (12)$$

and taking  $z = 7.1 \times 10^{-5}$  as the ratio between the light intensity of the global illumination for the iv-curve measurement and the local LASER illumination one can correct for this error. The result is shown as the second curve in **Fig. 10**, showing a nearly perfect constant value for the ratio of the serial resistances extracted from the CELLO maps and the global iv-curve. Similar corrections can be used to correct for the slope in the ratio of the diode resistances shown in **Fig. 11**.

One important consequence of this comparison of resistance data, i.e. slopes if analyzing iv-curves and averages if analyzing CELLO resistance maps, is that there are by now well understood scaling factors, which allow to translate data between both types of measurements.

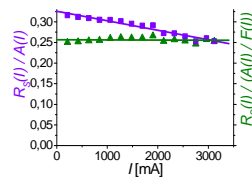


**Figure 10:** Squares:  $R_S(I)/A(I)$  vs.  $I$ , triangles:  $R_S(I)/(A(I)/F(I))$  vs.  $I$ .

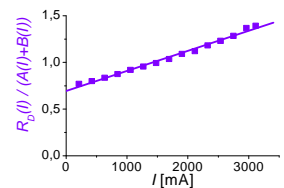


**Figure 11:**  $R_D(I)/(A(I)+B(I))$  vs.  $I$ .

Therefore two different approaches can be used to get quantitative numbers for the influence of defect types identified in CELLO maps on the iv-curve:

1. Calculate relative changes in averages of maps; they translate into corresponding relative changes in the slope of the global iv-curve. This is the standard procedure to analyze CELLO current and voltage maps at the working point of the solar cell [3].
2. Use values extracted from the global iv-curve as calibration values to get quantitative maps for several local parameter. This is the standard CELLO procedure for generating serial resistance maps [1].

A second important consequence is related to the interpretation of global iv-curves. If the distributed serial resistance as described in this paper is not taken into account, no correct interpretation is possible. The numbers extracted by fitting not only do not give good numbers for  $R_S$  but unrealistic values especially of the non-ideality factor  $n_{02}$  will result. The authors are convinced that whenever a large non ideality factor  $n_{02} \gg 2$  is found, this is almost certainly a consequence of the wrong interpretation of the serial resistance network of the solar cell and not related to properties of the pn-junction of the second diode.

#### 4 SUMMARY AND OUTLOOK

At least for commercially available solar cells nobody will design a perfect grid, leading to a (nearly) perfect equipotential layer across the solar cell. This is not necessary and much too expensive. As a consequence this non perfect equipotential layer, i.e. the distributed serial resistance must be taken into account. A formerly proposed model leading to Eq. (1) is necessary to get consistent results from IV-curve analysis and CELLO resistance maps. Necessary corrections between iv-curve analysis and CELLO measurements are taken into account. Different flow directions of the currents lead to an offset in the CELLO data and the usage of 4 reference electrodes used by CELLO leads to a 4 times larger serial resistance value.

The measurements presented here are just one example from a large number of CELLO measurements; they all give consistent results when taking into account the distributed serial resistance. This is probably true for all measurement tools sensitive to the local serial resistance. For further confirmation of the validity of Eq. (1) experiments like current-voltage impedance analysis along the IV-curve will be performed.

#### 5 REFERENCES

- [1] J. Carstensen, A. Schütt, and H. Föll, in *Proceedings of the 22nd European Photovoltaic Solar Energy Conference*, 1CV.1.34, Milan (2007).
- [2] J. Carstensen, A. Schütt, and H. Föll, in *Proceedings of the 23rd European Photovoltaic Solar Energy Conference*, 1CV.1.38, Valencia (2008).
- [3] J. Carstensen, S. Mathijssen, G. Popkirov, and H. Föll, in *Proceedings of the 20th European Photovoltaic Solar Energy Conference*, 1AV.2.40, Barcelona (2005).